ChemComm

Cite this: *Chem. Commun.*, 2012, **48**, 9586–9588

www.rsc.org/chemcomm

COMMUNICATION

Bipolar AIE-active luminogens comprised of an oxadiazole core and terminal TPE moieties as a new type of host for doped electroluminescence†

Jing Huang,[a] Xiao Yang,[b] Xianjie Li,[c] Pengyu Chen,[a] Runli Tang,[a] Feng Li,[c] Ping Lu,[c] Yuguang Ma,[c] Lei Wang,*[b] Jingui Qin,[a] Qianqian Li[a] and Zhen Li*[a]

Received 11th July 2012, Accepted 6th August 2012
DOI: 10.1039/c2cc34966c

For the first time, two bipolar AIE-active luminogens (Oxa-*p*TPE and Oxa-*m*TPE) constructed from tetraphenylethene and oxadiazole were utilized as fluorescence host materials in sky-blue doped OLEDs and exhibited high efficiencies with $L_{\max}$, $\eta_{C,\max}$, $\eta_{P,\max}$ and $\eta_{ext,\max}$ of 10 070 cd m^{-2}, 9.79 cd A^{-1}, 9.92 lm W^{-1} and 5.0%, respectively, broadening the scope for the utilization of AIE materials in the optoelectronic field.

The intriguing phenomenon of aggregation-induced emission (AIE),[1] first reported by Tang *et al.* in 2001, has been demonstrated as an effective way to tackle the notorious aggregation-caused quenching (ACQ) effect[2] and has aroused a new research topic of AIE materials, with tetraphenylethene (TPE) as a prototype AIE molecule for its facile synthesis and thermal stability.[3] Recently, lots of research work on TPE-based luminogens was reported with excellent electroluminescence characteristics (Chart S1, ESI†).[4] However, good blue light-emitting OLEDs utilizing AIE materials are still very scarce, though the lack of highly efficient blue light emitting materials caused by their intrinsic wide-band-gap nature is a critical drawback to realize full color displays.[5] The key feature of AIE luminophores is that the aggregation could block the non-radiative path, thus contributing to the efficient emission.[1b,6] This feature, really, is almost the same as one of the basic requirements for a good host in the guest–host systems, which is another effective approach to achieve high performance of LED devices.[7] Thus, is it possible to utilize the AIE materials as hosts, instead of their general role as emission layers, to achieve good OLEDs with blue emission? Once the efficient transfer of energy and charge from the AIE host to the dopant successfully occurs, the resultant OLED devices should exhibit good performance as expected.

As the first attempt, we still would like to obtain efficient blue light emitting OLEDs. Considering all the AIE molecules in our hands and reported by other scientists, TPE, with a band gap as large as 3.76 eV, was selected to realize our idea. Unfortunately, our experimental results disclosed that TPE is hole-dominated, since its hole mobility (~10^{-4} cm^2 V^{-1} s^{-1}) is one order-of-magnitude higher than its electron mobility (~10^{-5} cm^2 V^{-1} s^{-1}). This indicated that the direct usage of TPE as the host could not achieve the balance of the hole and electron injection. Accordingly, oxadiazole is chosen as the co-block to build new AIE hosts, due to its good electron-transporting property (Chart S2, ESI†).[8] Thus, two new AIE luminogens, **Oxa-*p*TPE** and **Oxa-*m*TPE**, were designed, as the potential good hosts (Chart 1). Also, BUBD-1, a frequently used sky blue fluorescent dopant, was utilized as the guest in this research.[9]

The synthetic routes to **Oxa-*p*TPE** and **Oxa-*m*TPE** are illustrated in Scheme S1 (ESI†) and the detailed procedures are presented in the ESI.† The thermal properties of **Oxa-*p*TPE** and **Oxa-*m*TPE** were investigated by thermal gravimetric analyses (TGA) and differential scanning calorimetry (DSC) (Fig. S1, ESI†). Their thermal-decomposition temperatures (T_d, corresponding to 5% weight loss) were determined to be about 414 and 400 °C, respectively. Owing to the more planar conformation, **Oxa-*p*TPE** possessed higher thermal stability and higher glass transition temperature (T_g) of 113 °C, compared to **Oxa-*m*TPE** with a T_g value of 103 °C.

Oxa-*p*TPE and **Oxa-*m*TPE** show absorption maxima at 320 and 302 nm, respectively (Fig. S2, ESI†), indicating that

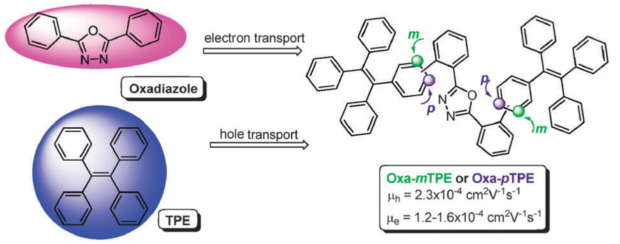

Chart 1 Chemical structures of **Oxa-*m*TPE** and **Oxa-*p*TPE**.

---

[a] *Department of Chemistry, Hubei Key Lab on Organic and Polymeric Opto-Electronic Materials, Wuhan University, Wuhan 430072, China. E-mail: lizhen@whu.edu.cn; Fax: +86-27-68755363; Tel: +86-27-68755363*

[b] *Wuhan National Laboratory for Optoelectronics, School of Optoelectronic Science and Engineering, Huazhong University of Science and Technology, Wuhan 430074, China. E-mail: lei96wang@163.com*

[c] *State Key Laboratory of Supramolecular Structure and Materials, Department of Chemistry, Jilin University, Jilin 130022, China*

† Electronic supplementary information (ESI) available: Experimental section and characterization data for **Oxa-*p*TPE** and **Oxa-*m*TPE**. CCDC 883924. For ESI and crystallographic data in CIF or other electronic format see DOI: 10.1039/c2cc34966c

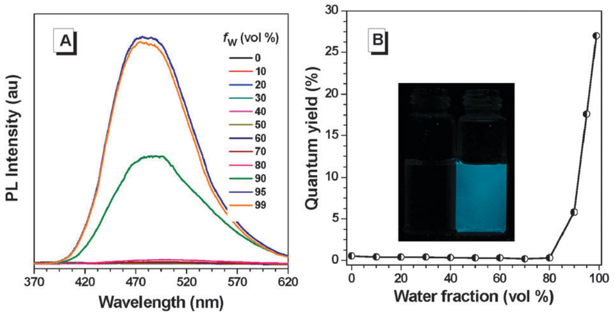

Fig. 1 (A) PL spectra of **Oxa-*p*TPE** in THF–H_2O mixtures with different water fractions (f_w). Concentration (μM): 10.7; excitation wavelength (nm): 320. (B) Plots of fluorescence quantum yields determined in THF–H_2O solutions using 9,10-diphenylanthracene (Φ = 90% in cyclohexane) as standard *versus* water fractions. Inset in (B): photos of **Oxa-*p*TPE** in THF–water mixtures (f_w = 0 and 99%) taken under the illumination of a 365 nm UV lamp.

the former is more conjugated than the latter, as a result of the *meta*- or *para*-linkage of TPE and oxadiazole unit. To investigate the possible AIE characteristics of these two dyes, their fluorescent behaviors were studied. Considering that the good and poor solvents should be well miscible, tetrahydrofuran and water were chosen as the solvent pair. Fig. 1 demonstrates the PL change and fluorescent image of **Oxa-*p*TPE** in THF and THF–water mixtures. It is easily seen that for dilute THF solution, the PL curve is practically a flat line parallel to the abscissa, confirming that it is nearly nonemissive in the solution state. However, when a large amount of water is added, intense emission is observed. As shown in Fig. 1, when the water fraction is over 80%, the PL intensity increases swiftly, indicating the formation of the aggregates. At a f_w value of 95%, the PL spectrum peak is at 479 nm for **Oxa-*p*TPE**, and the PL intensity is 120-fold higher than that in pure THF. Similar behavior was observed for **Oxa-*m*TPE** (Fig. S3, ESI†). The quantitative enhancement of emission was evaluated by the PL quantum yields (Φ_F), using 9,10-diphenylanthracene as the standard. From pure solution in THF to aggregate states in 95% or 99% aqueous mixtures, the Φ_F values for **Oxa-*p*TPE** and **Oxa-*m*TPE** increase from 0.0052 and 0.0044 to 0.27 and 0.346. Evidently, these two dyes are AIE-active.

To further understand the structure–property relationship at the molecular level, Density Functional Theory (DFT) calculations (B3LYP/6-31g*) were carried out. As shown in Fig. S4 (ESI†), the LUMOs of both molecules are located on the electron-accepting oxadiazole unit and the HOMO orbitals are mainly distributed on the TPE moiety, showing the almost separation of HOMO and LUMO orbitals. Fortunately, we have obtained the single crystal of **Oxa-*m*TPE**. As shown in Fig. S4 (ESI†), **Oxa-*m*TPE** has a twisted conformation and no intermolecular interactions are found in the packing arrangement, which is beneficial to prevent the formation of species detrimental to emission. This should be one advantage of these AIE molecules when used as hosts.

In order to obtain the carriers' mobilities of TPE, **Oxa-*p*TPE** and **Oxa-*m*TPE**, we used the time-of-flight (TOF) transient photocurrent technique. The carrier transit times t_T were evaluated from the intersection point of two asymptotes in the double logarithmic representations of the TOF transits (Fig. S5 and S6, inset (ESI†)). The carrier mobilities of **Oxa-*p*TPE**, **Oxa-*m*TPE** and TPE *versus* $E^{1/2}$ are shown in Fig. 2. Obviously, the electron mobility of the new fluorophores (1.2–1.6 × 10^{-4} cm^2 V^{-1} s^{-1}) is one order-of-magnitude higher than that of TPE (~10^{-5} cm^2 V^{-1} s^{-1}) by introducing the widely used oxadiazole unit, while the hole mobilities are of the same order of magnitude (~10^{-4} cm^2 V^{-1} s^{-1}) as TPE, which demonstrate their ambipolar property. This is beneficial for the dual charge transport and recombination in the diode structure, and also well realized our molecular design.

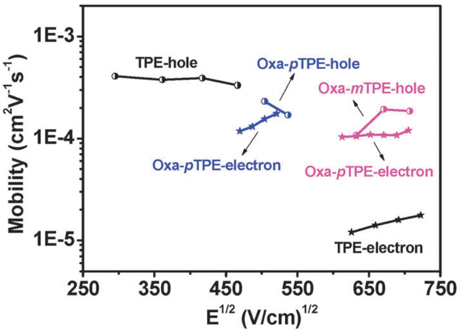

Fig. 2 Electron and hole mobilities *versus* $E^{1/2}$ for **TPE**, **Oxa-*p*TPE** and **Oxa-*m*TPE**.

The good thermal property, efficient solid-state emission and bipolar characteristics encouraged us to investigate the EL performance of **Oxa-*p*TPE** and **Oxa-*m*TPE** as host materials. As shown in Fig. 3, the spectral overlap between the PL spectra of the thin solid films of **Oxa-*p*TPE** and **Oxa-*m*TPE** and the BUBD-1 absorption spectrum indicates the efficient Förster energy transfer between them. Thus, we fabricated doped multilayer organic light-emitting diodes (OLEDs) with configurations of ITO–NPB (10 nm)/**Oxa-*p*TPE** or **Oxa-*m*TPE**: *x*% BUBD-1 (40 nm)/TPBi (10 nm)/Alq_3 (20 nm)/Al (100 nm). In these OLED devices, 1,4-bis(1-naphthylphenylamino)-biphenyl (NPB), 1,3,5-tris(*N*-phenylbenzimidazol-2-yl)benzene (TPBI) and tris(8-hydroxyquinolinato)aluminium (Alq_3) were used as hole-transporting, hole-blocking and electron-transporting layers, respectively, **Oxa-*p*TPE** and **Oxa-*m*TPE** served as host materials and BUBD-1 was the dopant. The energy gap of BUBD-1 with a lowest unoccupied molecular orbital/highest occupied molecular orbital level of 2.6/5.1 eV is well confined

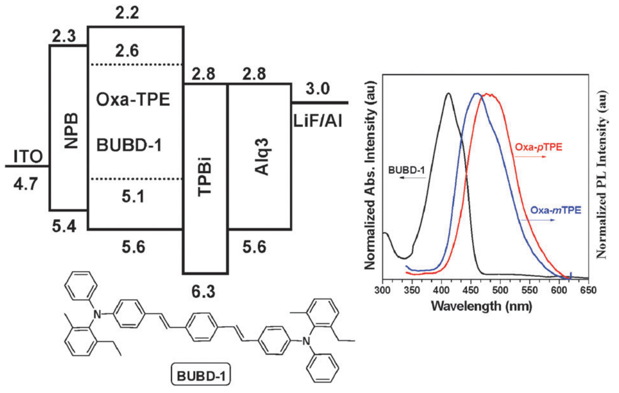

Fig. 3 Left: energy level diagrams and configurations of sky blue-doped EL devices of **Oxa-*p*TPE** and **Oxa-*m*TPE**. Abbreviations: NPB = 4,4-bis(1-naphthylphenylamino)biphenyl, TPBi = 1,3,5-tris(*N*-phenyl-benzimidazol-2-yl)benzene and Alq_3 = tris(8-hydroxyquinolinato)-aluminium. Right: UV spectrum of BUBD-1 in dilute solution and PL spectra of solid thin films of **Oxa-*p*TPE** and **Oxa-*m*TPE**.

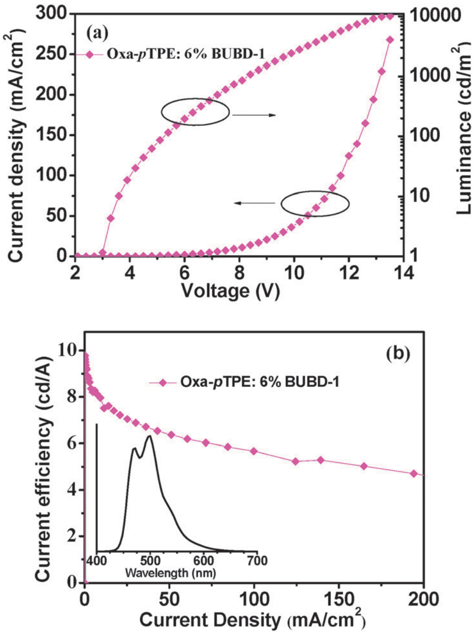

Fig. 4 Changes in (a) current density and luminance with the applied voltage and (b) current efficiency with the current density in BUBD-1 doped multilayer EL devices of **Oxa-*p*TPE**. Inset in panel (b): EL spectrum of the device. Device configuration: ITO/NPB (10 nm)/**Oxa-*p*TPE**: 6% BUBD-1 (40 nm)/TPBi (10 nm)/Alq$_3$ (20 nm)/Al (100 nm).

in **Oxa-*p*TPE** or **Oxa-*m*TPE** from the energy level diagram (Fig. 3). In addition, we observed that the LUMO of BUBD-1 is close to the energy level of cathode Al, enough to cause electron trapping, and the HOMOs of **Oxa-*p*TPE** and **Oxa-*m*TPE** are close to the hole transport material NPB, beneficial for transporting holes to the host. The detailed EL performances of the devices are summarized in Table S2 (ESI†).

The optimal BUBD-1-doped concentration is 6% for **Oxa-*p*TPE** and 3% for **Oxa-*m*TPE**. The EL spectra are shown in Fig. 4 (b, inset) and Fig. S7 and S8 (b, inset, ESI†). The doped devices exhibit sky blue emission due to the dopant BUBD-1 fluorescence and the CIE$_{x,y}$ coordinates are (0.15, 0.34) and (0.15, 0.33), respectively. As shown in Fig. 4 and Fig. S7 (ESI†), the devices turned on at a voltage of 5.1 V for **Oxa-*p*TPE** and 6.25 V for **Oxa-*m*TPE**. Accompanying the increase in the voltage, the luminance increased rapidly. The doped device based on **Oxa-*m*TPE** exhibits a maximum luminance ($L_{\max}$) of 7734 cd m^{-2}, a maximum current efficiency ($\eta_{\mathrm{C,max}}$) of 9.82 cd A^{-1} and a maximum power efficiency ($\eta_{\mathrm{P,max}}$) of 7.96 lm W^{-1}. Better EL performance is observed for **Oxa-*p*TPE** with $L_{\max}$, $\eta_{\mathrm{C,max}}$ and $\eta_{\mathrm{P,max}}$ of 10 070 cd m^{-2}, 9.79 cd A^{-1} and 9.92 lm W^{-1}, respectively. Noteworthily, the highest external quantum efficiency reaches 5.0%, which illustrates the excellent carrier recombination as well as the balance of holes and electrons in the emissive layer. The satisfactory EL data could be explained as follows: on the one hand, when fabricated as thin films, the intramolecular rotation of the two AIE-active hosts is restricted, which blocks the non-radiative path and efficiently transfers charge and energy from the host to the dopant *via* radiative decay; on the other hand, the bulky nonplanar TPE moieties attached to the oxadiazole unit effectively suppress intermolecular interactions and alleviate self-quenching of the dopant.

In summary, bipolar AIE-active luminogens **Oxa-*p*TPE** and **Oxa-*m*TPE** were successfully synthesized and served as fluorescence host materials in sky-blue doped OLED devices with the aim of improving the EL performance. Thanks to the bipolar characteristic and specific AIE feature, efficient charge and energy transfer from **Oxa-*p*TPE** and **Oxa-*m*TPE** to dopant BUBD-1 occurred *via* radiative decay in the emissive layer. The doped devices exhibit high efficiencies with $L_{\max}$, $\eta_{\mathrm{C,max}}$, $\eta_{\mathrm{P,max}}$ and $\eta_{\mathrm{ext,max}}$ of 10 070 cd m^{-2}, 9.79 cd A^{-1}, 9.92 lm W^{-1} and 5.0%, which demonstrate that AIE molecules are promising host materials for blue-emitting OLED applications. Thus, our preliminary results might open up a new avenue for the utilization of AIE materials in the photonic and electronic research field.

This work was supported by the National Science Foundation of China (no. 21161160556). Z. Li thanks the support of Open Project of State Key Laboratory of Supramolecular Structure and Materials (sklssm201219).

Notes and references

1 (*a*) J. Luo, Z. Xie, J. W. Y. Lam, L. Cheng, H. Chen, C. Qiu, H. S. Kwok, X. Zhan, Y. Liu, D. Zhu and B. Z. Tang, *Chem. Commun.*, 2001, 1740; (*b*) Y. Hong, J. W. Y. Lam and B. Z. Tang, *Chem. Commun.*, 2009, 4332.

2 A. C. Grimsdale, K. L. Chan, R. E. Martin, P. G. Jokisz and A. B. Holmes, *Chem. Rev.*, 2009, **109**, 897.

3 (*a*) Y. Dong, J. W. Y. Lam, A. Qin, J. Liu, Z. Li, B. Z. Tang, J. Sun and H. S. Kwok, *Appl. Phys. Lett.*, 2007, **91**, 011111; (*b*) J. Huang, X. Yang, J. Wang, C. Zhong, L. Wang, J. Qin and Z. Li, *J. Mater. Chem.*, 2012, **22**, 2478; (*c*) J. Huang, N. Sun, J. Yang, R. Tang, Q. Li, D. Ma, J. Qin and Z. Li, *J. Mater. Chem.*, 2012, **22**, 12001; (*d*) Y. Yang, X. Su, C. N. Carroll and I. Aprahamian, *Chem. Sci.*, 2012, **3**, 610; (*e*) N. W. Tesng, J. Liu, J. C. K. Ng, J. W. Y. Lam, H. H. Y. Sung, I. D. Williams and B. Z. Tang, *Chem. Sci.*, 2012, **3**, 493; (*f*) S. Chen, J. Liu, Y. Liu, H. Su, Y. Hong, C. K. W. Jim, R. T. K. Kwok, N. Zhao, W. Qin, J. W. Y. Lam, K. S. Wong and B. Z. Tang, *Chem. Sci.*, 2012, **3**, 1804.

4 (*a*) W. Z. Yuan, P. Lu, S. Chen, J. W. Y. Lam, Z. Wang, Y. Liu, H. S. Kowk, Y. Ma and B. Z. Tang, *Adv. Mater.*, 2010, **22**, 2159; (*b*) Z. Zhao, S. Chen, X. Shen, F. Mahtab, Y. Yu, P. Lu, J. W. Y. Lam, H. S. Kwok and B. Z. Tang, *Chem. Commun.*, 2010, **46**, 686; (*c*) Z. Zhao, J. W. Y. Lam, C. Y. K. Chan, S. Chen, J. Liu, P. Lu, M. Rodriguez, J. L. Maldonado, G. Ramos-Ortiz, H. H. Y. Sung, I. D. Williams, H. Su, K. S. Wong, Y. Ma, H. S. Kwok, H. Qiu and B. Z. Tang, *Adv. Mater.*, 2011, **23**, 5430; (*d*) C. Y. K. Chan, Z. Zhao, J. W. Y. Lam, J. Liu, S. Chen, P. Lu, F. Mahtab, X. Chen, H. H. Y. Sung, H. S. Kwok, Y. Ma, I. D. Williams, K. S. Wong and B. Z. Tang, *Adv. Funct. Mater.*, 2012, **22**, 378.

5 (*a*) R. J. Tseng, R. C. Chiechi, F. Wudl and Y. Yang, *Appl. Phys. Lett.*, 2010, **88**, 093512; (*b*) K. T. Kamtekar, A. P. Monkman and M. R. Bryce, *Adv. Mater.*, 2010, **22**, 572.

6 (*a*) J. Chen, B. Xu, X. Ouyang, B. Z. Tang and Y. Cao, *J. Phys. Chem. A*, 2004, **108**, 7522; (*b*) Z. Li, Y. Dong, B. Mi, Y. Tang, H. Tong, P. Dong, J. W. Y. Lam, Y. Ren, H. H. Y. Sun, K. Wong, P. Gao, I. D. Williams, H. S. Kwok and B. Z. Tang, *J. Phys. Chem. B*, 2005, **109**, 10061; (*c*) Y. Ren, J. W. Y. Lam, Y. Dong, B. Z. Tang and K. S. Wong, *J. Phys. Chem. B*, 2005, **109**, 1135.

7 J. Shi and C. W. Tang, *Appl. Phys. Lett.*, 2002, **80**, 3201.

8 (*a*) G. Hughes and M. R. Bryce, *J. Mater. Chem.*, 2005, **15**, 94; (*b*) W. Y. Wong, Z. He, S. H. So, K. L. Tong and Z. Lin, *Organometallics*, 2005, **24**, 4079; (*c*) Z. He, W. Y. Wong, X. Yu, H. S. Kwok and Z. Lin, *Inorg. Chem.*, 2006, **45**, 10922.

9 M. Lin, L. Wang and W. K. Wong, *Appl. Phys. Lett.*, 2006, **89**, 121913.